20th Australasian Fluid Mechanics Conference
Perth, Australia
5-8 December 2016

Direct Numerical Simulation of a Row of Impinging Jets

Keita JINNO[1], Koichi TSUJIMOTO[1], Toshihiko SHAKOUCHI[1] and Toshitake ANDO[1]

[1]Division of Mechanical Engineering
Mie University, Kurimamachiya-cho 1577, Tsu, Mie, 514-8507 Japan

Abstract

In order to improve the performance of heat transfer with multiple impinging jets (MIJ), we investigate the DNS (direct numerical simulation) of four round impinging jets arranged in a row at an inflow of flow field. As a geometrical parameter, a separation between each jet is varied. From view of instantaneous vortical structures and time-averaged velocity distribution, it reveals that the generation of vortical structures are enhanced due to an interaction between each jet and that various type of upward flow appears according to the separation between each jet. In addition to improve the heat transfer performance of MIJ, an active control of transverse oscillation of MIJ is conducted. Compared to the uncontrolled case, it is revealed that the total heat transfer rate is improved at a specific oscillating frequency through the transverse oscillation.

Introduction

Impinging jet is widely used for cooling of industrial applications such as electric device, blades of gas turbine, hot steel and so on, since it possesses high performance of heat transfer rate and is easier to implement into various system. Their characteristics are reviewed by a few notable literatures [2, 7]: impinging jets are subdivided into three regions, such as free jet region, stagnation region and wall jet region; the performance of heat transfer on the impinging wall is depending on the Re number, the shape of nozzle, the number of nozzle, the distance between the nozzle and the impinging wall and so on. Further a single impinging jet produces a high heat transfer rate around an impinging position on an impinging wall, while the heat transfer performance decays increasing distance from the impinging position. Thus in order to overcome the shortcoming of single impinging jet such as the occurrence of both inhomogeneous heat distribution on the wall and the narrow heating area, multiple impinging jets (MIJ) are generally introduced in industrial applications. Thus far foe MIJ, it is well-known that each jet of MIJ interacts with each other, producing the complex flow field [1, 8]. In addition, the heat transfer performance is significantly influenced with their interaction. Therefore to realize an optimum heat transfer performance, the influence of geometrical parameter of jets, *i.e.*, the arrangement pattern should be investigated. In the present paper, to improve the performance of heat transfer with MIJ in which four round impinging jets arranged in a row at an inflow of flow field, we investigate the performance using DNS (direct numerical simulation). As a geometrical parameter, a separation length between each jet is varied. In addition, to improve the heat transfer performance of MIJ, an active control in which the transverse oscillation with sine function is examined for the case having lowest heat transfer performance among the examined cases.

Numerical method

Governing equations and their discretization

Under the assumption of incompressible flow, the governing equations are as follows:

$$\frac{\partial u_i}{\partial x_i} = 0 \tag{1}$$

$$\frac{\partial u_i}{\partial t} + h_i = -\frac{\partial p}{\partial x_i} + \frac{1}{\mathrm{Re}}\frac{\partial^2 u_i}{\partial x_j \partial x_j} \tag{2}$$

$$(h_i = \varepsilon_{ijk}\omega_j u_k, \omega_j : \text{vorticity})$$

$$\frac{\partial T}{\partial t} + u_i\frac{\partial T}{\partial x_i} = \frac{1}{\mathrm{RePr}}\frac{\partial^2 T}{\partial x_j \partial x_j} \tag{3}$$

where u_i is velocity component, p is total pressure, T is temperature and ε_{ijk} is Levi-Civita symbol. The convective terms of equation (2) is described as rotational form. Above equations are normalized by both the diameter of the inlet jet, D and the inlet velocity, V_0. Re number and Pr number are defined as $\mathrm{Re} = V_0 D/\nu$ (ν: dynamic viscosity) and $\mathrm{Pr} = \nu/\alpha$ (α: thermal conductivity), respectively. The computational volume is the rectangular box. The origin of axes is set at the center of an impinging wall. The wall-normal direction, $y(= x_2)$ and two horizontal directions, $x(= x_1)$, $z(= x_3)$ are set, and the velocity component for each direction denotes $u(= u_1)$, $v(= u_2)$ and $w(= u_3)$, respectively. Similarly, the radial direction, r, the azimuthal direction, θ are defined, and the velocity components for two directions denote as u_r, u_θ, respectively.
The spatial discretization is performed with sine or cosine series expansion in x and z directions and 6th-order compact scheme [3] in y direction. In order to remove the numerical instability due to the nonlinear terms, the 2/3-rule is applied for the horizontal directions and an implicit filtering for the wall-normal direction is conducted with 6th order compact scheme. For the time advancement, third order Adams-Bashforth method is used. The well-known MAC method is employed for pressure-velocity coupling, which results in a Poisson equation for the pressure. After the Poisson equation is expanded with sine series in x and z directions, the independent differential equations are obtained for each wave number and then is discretized with sixth order compact scheme. Finally, the penta-diagonal matrix is deduced for each wave number. In the present simulation code, these matrices are solved using the LU Decomposition method. When vortical structures approaches the side boundary of impinging wall, relatively strong low-pressure regions being formed by vortical structures do not meet the pressure boundary condition, *i.e.* $p = 0$. In the present simulation, since the spectral method is used, the occurrence of this discrepancy at the side boundary induces the unphysical numerical oscillation in the whole flow field. Thus the vortical motions should be artificially reduced near the boundary. In the present simulation, a fringe (buffer) region [4] is introduced around side boundary in order to reduce the perturbation using an appropriate external force.

Calculation conditions

The inlet velocity distribution is assumed to be top-hat type, which is given as follows:

$$V_{in}(r) = \frac{V_0}{2} - \frac{V_0}{2}\tanh\left[\frac{1}{4}\frac{R}{\theta_0}\left(\frac{r}{R} - \frac{R}{r}\right)\right] \tag{4}$$

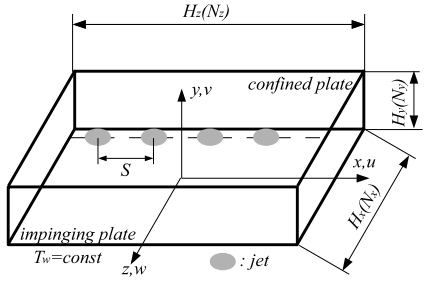

Figure 1: Coordinate system and computational domain

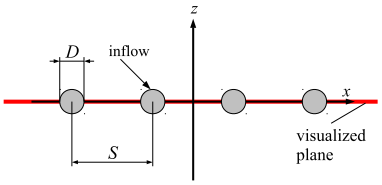

Figure 2: Geometrical arrangements of nozzles

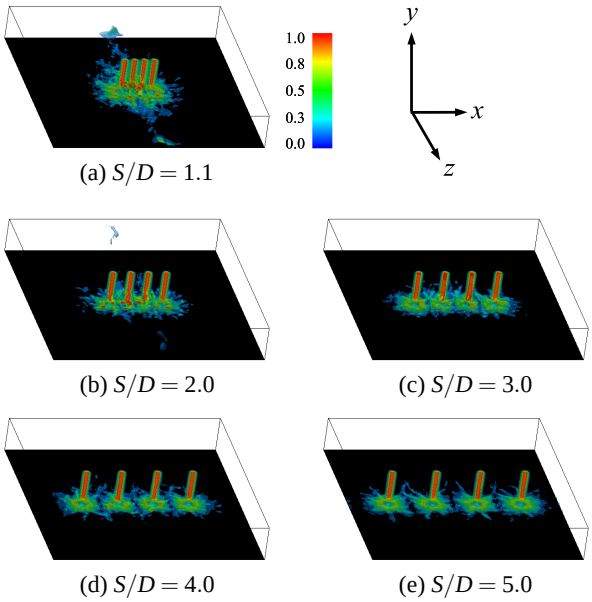

(a) $S/D = 1.1$ (b) $S/D = 2.0$ (c) $S/D = 3.0$ (d) $S/D = 4.0$ (e) $S/D = 5.0$

Figure 3: Contour of instantaneous velocity magnitude

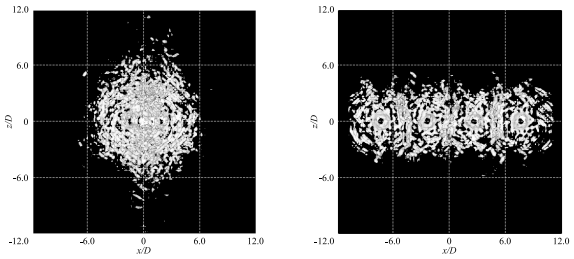

(a) $S/D = 1.1$ (b) $S/D = 5.0$

Figure 4: Instantaneous vortex structures

where, V_0 is the center velocity. θ_0 denotes the initial momentum thickness, $R(= D/2)$ is radius of an inlet jet. This inlet velocity profile is selected by referring to the literature [5]. $(R/\theta_0 = 20)$. In the present simulations, the distance to the impinging wall, H is $H/D = 4$. Figure 1 shows the computational volume and coordinate systems. Computational conditions such as the size of computational domain, the grid number, the Reynolds number, the Prandtl number is $(H_x, H_y, H_z) = (24D, 4D, 24D)$, $(N_x, N_y, N_z) = (128, 100, 128)$, Re $= 1500$ and Pr $= 0.71$, respectively. The grid spacing of wall-normal direction is densely populated near wall region. The inflow temperature, T_0 and the ambient temperature, T_a are assumed to be higher than the wall temperature, T_w, *i.e.*, $T_0 = T_a > T_w$. The statistical properties are averaged over the time and azimuthal direction. The mean quantity is denoted with bar $(\overline{\ })$ and fluctuating components, by prime $(')$. In the present study, we calculate the conditions where the jets are arranged in a row as shown in figure 2, so we compare the effect on the flow structures and heat transfer performance due to the separation between each jet. The separation between each jet S is varied as $S/D = 1.1 \sim 5.0$ (five cases are conducted). Moreover we introduce a transversing oscillating control for the case of the most heat transfer performance was lower in five separations between each jet. For details and the results of oscillating control will be described later.

Results and discussions

flow structures

The instantaneous contours of velocity magnitude for all cases are visualized in figures 3. It is observed that each jet impinges and then spreads over on the impinging wall, and further collides with each other on the impinging wall. As the separation length between jets S increases, the structures of each jet is similar to that of a single impinging jet. On the other hand, in the narrower cases ($S/D = 1.1, 2.0$) as soon as the jet impinges, the flow is deflected perpendicular to the row direction. Figures 4 show the instantaneous vortex structures visualized by the isosurfaces of second invariant velocity gradient tensor, $Q(= 0.3)$ in the cases of $S/D = 1.1$ and 5.0. For the wider case (figure 4 (b)), the vortex structures are densely populated around the impinging positions and the positions between them, while for the narrower case (figure 4 (a)), the fine vortices are actively formed and spread in z-direction as well as the velocity magnitude shown in figure 3 (a).

The contours of time-averaged velocity for the case of $S/D = 1.1, 2.0$ and 5.0 on the $x-y$ plane through the center of jets are shown in figures 5. It is observed that the stagnation regions around the impingement point and the upward flow due to collision of each wall jet are formed. Depending on the decreasing the separation length S, the potential core length of individual jet is shorter, *i. e.*, the breakdown in the free jet region proceeds before the impingement to the wall. In particular in the most narrower case of $S/D = 1.1$, the outer boundary of jet in the free jet region is immediately unstable near the inflow, and it start to collapse around the height of about $y/D = 2.0$ at $x/D = 0$.

Figures 6 show the contours of turbulent kinetic energy (TKE) on the $x-y$ plane at $S/D = 1.1, 2.0$ and 5.0. In the narrow case ($S/D = 1.1$), the peak value of TKE appears the area where the outer-edge of each jet interacts with the upwash flow. In the case of $S/D = 2.0$, the peak appears both the outer-edge of each jet and the center area at which the wall jet issued from each jet collide with each other. In the wide case ($S/D = 5.0$) the peaks around the outer-edge of jet disappear, but the peaks around collision point of wall jet only appears. From these findings, it is demonstrated that the interaction between upwash flow and each jet is dominant in the case of narrow separation length, however, as increasing the separation length, the interaction weakens, and the collision of wall jet is relatively dominant.

heat transfer characteristics

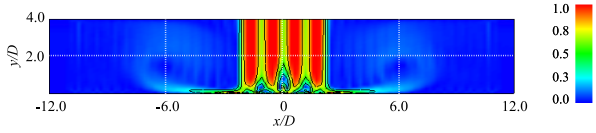

(a) $S/D = 1.1$

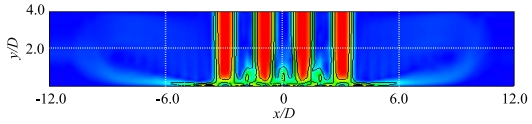

(b) $S/D = 2.0$

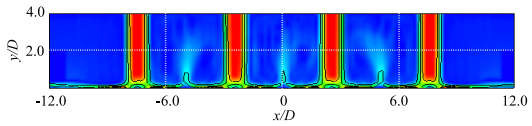

(c) $S/D = 5.0$

Figure 5: Contour of mean velocity magnitude

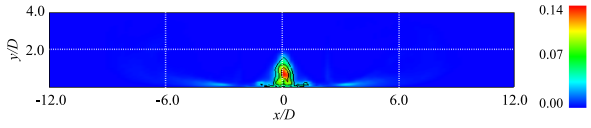

(a) $S/D = 1.1$

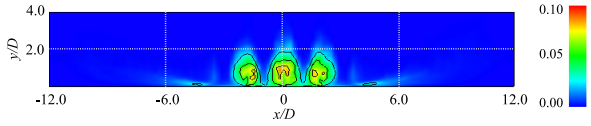

(b) $S/D = 2.0$

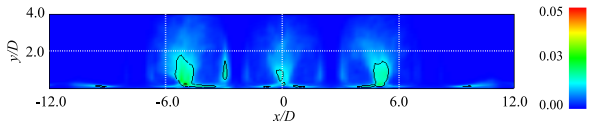

(c) $S/D = 5.0$

Figure 6: Contour of turbulent kinetic energy

The contours of time-averaged local Nu number on the impinging wall are shown in figures 7. In general, it is well-known that a single impinging jet produces high heat transfer around an impinging position and that the heat transfer decays increasing the distance from the impinging position. In the present results, although the jets is arranged in a row and interact with each other, the heat transfer performance around individual jet is qualitatively more similar to that of a single jet, as the separation length S increases. Note that as decreasing the separation S the peak value of Nu number increases, in particular, the peak value of $S/D = 1.1$ become about 1.5 times larger than that of other cases.

In order to quantitatively evaluate the heat transfer performance, the total Nu number by integrating local Nu number Nu_{sum} is shown in figure 8.

$$\mathrm{Nu}_{\mathrm{sum}} = 2\pi \int \mathrm{Nu} r dr \tag{5}$$

where r denotes the distance from the center of the impinging wall on the impinging plane. The total Nu number monotonically increases proportional to the integrated area. With taking a closer look at the detail of distribution, for small area ($r/D \leq 6.0$) the narrower separation ($S/D = 1.1$) is higher than the wider one while for the large area ($r/D \geq 6.0$) wider separation ($S/D = 4.0$ and 5.0) is superior to the narrower separation, suggesting that the efficiency of heat transfer at the

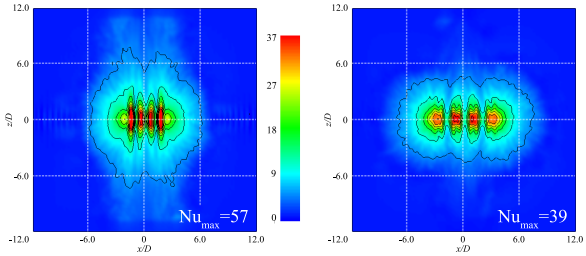

(a) $S/D = 1.1$ (b) $S/D = 2.0$

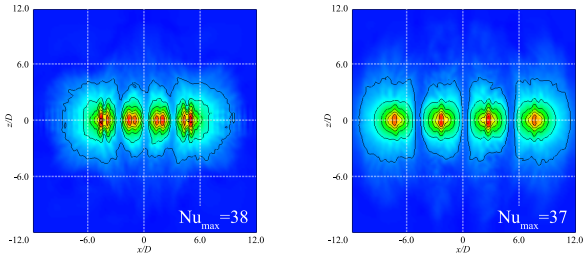

(c) $S/D = 3.0$ (d) $S/D = 5.0$

Figure 7: Contour of Nusselt number

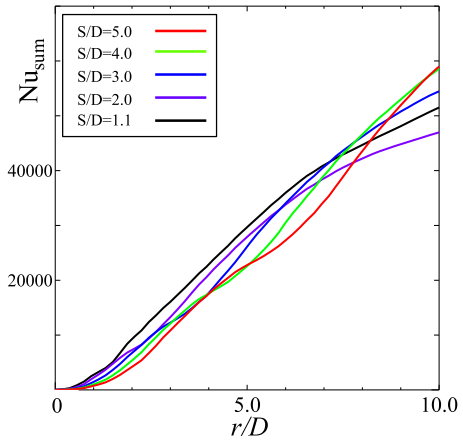

Figure 8: Summation of Nusselt number distribution

winder separation is recovered due to the reduction of the jet-jet interaction.

Transversing scillation control for jets

From the results described above, it is reconfirmed that both the reduction of heat transfer performance and inhomogeneous heat distribution on the impinging wall occur irrespective to the separation length S. Thus to improve the heat transfer performance, an active control method in which the jets transversely oscillates with sine function shown in figure 9 is examined for the case having lowest heat transfer performance ($S/D = 2.0$). As a control parameter, an amplitude of the oscillation A_c is set $A_c/D = S/D$, the oscillating frequency f varies as $f = 0.01, 0.02$, and 0.05. The instantaneous contours of velocity magnitude are visualized in figure 10. It is observed that each jet flow sweeps the impinging wall along the row direction, and that the impinging position is not fixed but continuously moves. Figures 11 show the contour of time-averaged local Nu number on the impinging wall. Compared to the uncontrolled case (figure 11 (a)), even in the case of oscillating control the occurrence of peak value still remains on the impinging wall, however, the low Nu number region between each jet founded in the uncontrolled MIJ disappears owing to the sweep motion of transverse oscillation. In addition since the sweep motion reduces the mag-

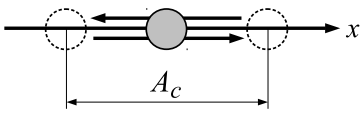

Figure 9: Transversing oscillation

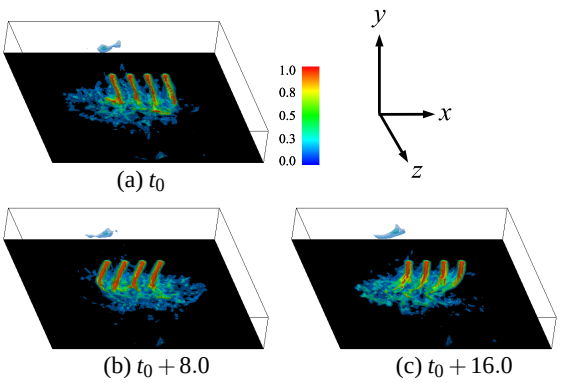

(a) t_0 (b) $t_0 + 8.0$ (c) $t_0 + 16.0$

Figure 10: Contour of instantaneous velocity magnitude ($f = 0.05$)

nitude of impinging velocity on the impinging wall, the peak value of Nu number is reduced compared to the uncontrolled MIJ. The distributions of total Nu number are shown in figure 12. All cases including the uncontrolled case demonstrate almost same distribution inside $r/D = 6.0$, however only the case of high frequency ($f = 0.05$) improves the heat transfer performance compared to the uncontrolled MIJ. At present we do not fully understand the reason why the improvement of heat transfer at high frequency case occurs, however from figure 11(d), since the weak heat transfer region around the impinging positions extends in z direction compared to the other frequency cases, it is considered that the high frequency control enhances the flow perpendicular to the row direction, contributing to the enhancement of summation of Nu number.

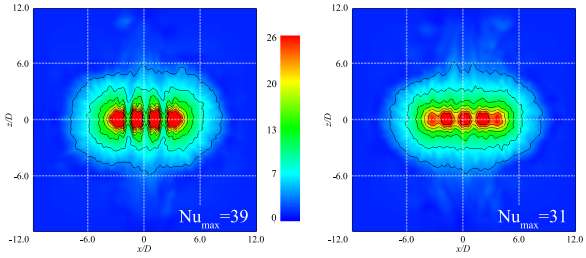

(a) uncontrolled (b) $f = 0.01$

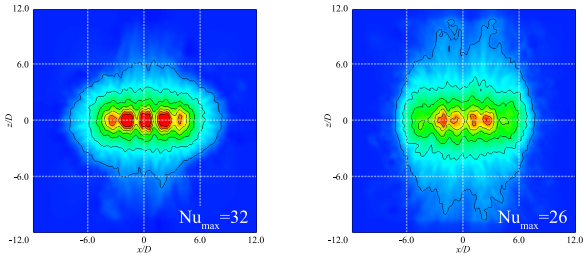

(c) $f = 0.02$ (d) $f = 0.05$

Figure 11: Contour of local Nusselt number

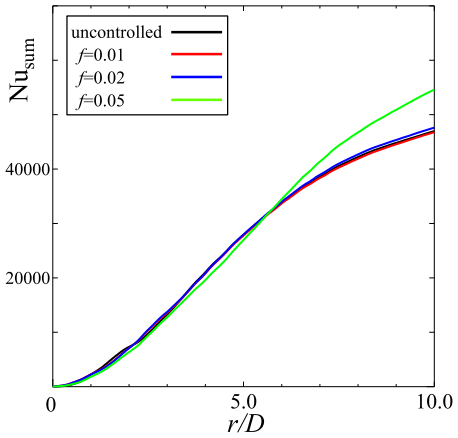

Figure 12: Summation of Nusselt number distribution

Conclusions

- From the instantaneous flow structures, it is revealed that upwash is formed due to the jet-jet interaction, and that the flow structures changes according to the separation between jets.
- From analysis of the heat transfer performance, it is observed that the heat transfer performance is strongly influenced by the flow structures due to the interaction between jets.
- From analysis of the heat transfer performance for the active controlled MIJ, it is revealed that the deterioration of heat transfer due to the jet-jet interaction is suppressed using the transverse oscillation, and that the total heat transfer rate is improved at a specific control frequency compared to that of the uncontrolled MIJ.

References

[1] Geers, L.F.G. Tummers, M.J., and Hanjalić, K., Particle imaging velocimetry-based identification of coherent structures in normally impinging multiple jets, *Physics Fluids*, **17**-5, 2005, 1-13.

[2] Kataoka, K., Impingement heat transfer augmentation due to large scale eddies, *In Heat Transfer 1990, Proc. 9th Int. Heat Transfer Conf.*, **1**, 1990, 255-273.

[3] Lele, S. K., Compact finite difference schemes with spectral-like resolution, *J. Comp. Phys.*, **103**, 1992, 16-42.

[4] Nordstrom, J., Nordin, N., and Henningson, D. S., The fringe region technique and the fourier method used in the direct numerical simulation of spatially evolving viscous flows, *SIAM J. Sci. Comp.*, **20**-4, 1999, 1365-1393.

[5] Silva, C. B. and Metais, O., Vortex control of bifurcating jets: A numerical study, *Phys. Fluids*, **14**, 2002, 3798-3819.

[6] Tsujimoto, K., Kariya, S., Shakouchi, T. and Ando, T., Investigation on Jet Mixing Rate Based on DNS of Excitation Jets, *Trans. JSME* , **74**-737B, 2008, 34-41.(in Japanese)

[7] Viskanta,R., Heat transfer to impinging isothermal gas and flame jets, *Exp. Therm. Fluid Sci.*,**6**, 1993, 111-134.

[8] Weigand, B. and Spring, S., Multiple jet impingement - a review, *Heat Transfer Res.*, **42**-2, 2011, 101-142.